Received: 23 November 2021 | Revised: 15 March 2022 | Accepted: 11 April 2022

DOI: 10.1002/pip.3565

RESEARCH ARTICLE

PROGRESS IN PHOTOVOLTAICS WILEY

Power conversion efficiency of 25.26% for silicon heterojunction solar cell with transition metal element doped indium oxide transparent conductive film as front electrode

Gangqiang Dong[1] | Jiacheng Sang[2] | Chen-Wei Peng[1] | Fengzhen Liu[2] | Yurong Zhou[2] | Cao Yu[1]

[1]Suzhou Maxwell Technologies Co., Ltd, Suzhou, China

[2]College of Materials Science and Opto-Electronic Technology, University of Chinese Academy of Sciences, Beijing, China

Correspondence
Yurong Zhou, College of Materials Science and Opto-Electronic Technology, University of Chinese Academy of Sciences, No. 19A Yuquan Road, Shijingshan District, Beijing 100049, China.
Email: zhouyurong@ucas.edu.cn

Cao Yu, Suzhou Maxwell Technologies Co., Ltd, No.1801 Pangjin Road, Wujiang Economic Development Zone, Suzhou, Jiangsu 215200, China.
Email: yucao@maxwell-gp.com.cn

Abstract

In this paper, to improve the power conversion efficiency (E_{ff}) of silicon heterojunction (SHJ) solar cells, we developed the indium oxide doped with transition metal elements (IMO) as front transparent conductive oxide (TCO) layer combined with microcrystalline silicon (μ-Si:H(n^+)) for SHJ solar cell. The optical and electrical properties as well as structures of hydrogenated IMO (IMO:H) films were studied and compared to conventional indium tin oxide (ITO) film. Such IMO:H films have high carrier mobility over 70 $cm^2/V{\cdot}s$, high transmittance, and low free carrier absorption, which leads to a high short circuit current density exceeding 40 mA/cm^2. In addition, the low sheet resistance and contact resistivity of the IMO:H films contribute to the high fill factor of the solar cell. The average E_{ff} of solar cells with IMO:H + μ-Si:H(n^+) is improved by 0.4% compared with that of the solar cells with ITO + a-Si:H(n^+). Finally, a certified efficiency up to 25.26% (total area, 274.5 cm^2) was achieved.

KEYWORDS
power conversion efficiency, short circuit current density, silicon heterojunction, transition metal elements, transparent conductive oxide

1 | INTRODUCTION

Silicon heterojunction (SHJ) solar cells, which combine a crystalline silicon (c-Si) absorber with hydrogenated amorphous silicon (a-Si:H) emitter and back-field layer, are the promising candidates for high efficiency solar cells.[1–3] A record power conversion efficiency (E_{ff}) of 26.6% for the c-Si solar cells with a single absorber was realized on the SHJ solar cells with an interdigitated back contact.[4] Due to the simple process and relatively high efficiency, SHJ solar cells with a front contact and back-junction structure are the mainstream. The E_{ff} of the bifacial SHJ solar cells has reached 25.11%,[5] which uses indium tin oxide (ITO) as transparent conductive oxide (TCO) layer.

Although the SHJ solar cell has advantages in high open-circuit voltages (V_{OC}), which is up to 750 mV due to low surface recombination,[2] it also has clear disadvantages on short circuit current density (J_{sc}) and contact resistance properties compared with tunnel oxide passivating contacts (TOPCon) solar cells. It is reported that the TOPCon solar cell has a high J_{sc} up to 42.5 mA/cm^2.[6] To improve the J_{sc} of SHJ solar cells while maintaining high fill factor, it is necessary to explore and develop TCO films with better optical and electrical properties. In the past decades, the ITO films have been grown by several deposition techniques, including direct current (DC) or radio-frequency sputtering,[7,8] thermal evaporation and electron beam evaporation,[9,10] plasma-enhanced reactive thermal evaporation,[11,12] pulsed laser deposition,[13,14] and reactive plasma deposition.[15] Among them, the sputtering process is currently the most widely used technique to deposit ITO films in mass production.

The parasitic absorption of the amorphous silicon layer and transparent conductive oxide films is the major obstacle for improving the device J_{sc} and performance.[16] Currently, the use of hydrogenated microcrystalline silicon (μ-Si:H) rather than hydrogenated amorphous silicon (a-Si:H) as a window layer and the improvement of the

transmission and mobility in TCO are the main research directions.[5] In order to optimize the conductivity, mobility and transmittance of TCO thin films, many growth conditions have been investigated. Enlarging the bandgap of TCO films is a preferable alternative to increase the transmittance.[16,17] Increasing the carrier concentration can improve the conductivity of TCO films. However, there exists large absorption induced by free carriers in the near-infrared (NIR) wavelength region,[7,18,19] which results in high light absorption within the TCO films. So, with the increasing carrier concentration in TCO films, they become less transparent as they become more conductive.[18] Thus, to balance the trade-off between transmittance and electrical conductivity of TCO films, the most feasible way is the manipulation of bandgap and mobility. The mobility of conventional ITO film is rather low (20–40 $cm^2/V{\cdot}s$) compared to theoretical values limited by ionized impurities. It is reported that hydrogen contained in the sputtering gas can reduce the density of scattering centers by reducing the oxygen deficient phases and the non-activated Sn dopants, which in turn improved the mobility.[7,8,18]

In this work, high-quality indium oxide doped with transition metal elements (IMO) thin films were deposited by sputtering process. The optical and electrical properties, such as absorption, sheet resistance, mobility, and contact resistivity, were optimized by varying hydrogen concentrations and stoichiometry. Its application in SHJ solar cells as front TCO layer was also explored. As a result, a 25.26% total area efficiency for SHJ solar cell with high J_{sc} exceeding 40 mA/cm^2 was achieved on 274.5cm^2 c-Si wafer.

2 | EXPERIMENTAL DETAILS

2.1 | TCO films

TCO thin films were deposited on textured silicon (100) wafers and glass substrates by DC sputtering. Two kinds of targets were used: ITO (In_2O_3:SnO_2 = 97:3 wt%) and indium oxide doped with transition metal (IMO). M is the abbreviation for titanium oxide (TiO_2), cerium oxide (CeO_2) and tantalum oxide (Ta_2O_5) with corresponding mass ratios of 0.22 wt% TiO_2, 0.14 wt% CeO_2, 0.03 wt% Ta_2O_5 in the target. The sputtering gases were pure argon, pure oxygen and argon–hydrogen mixture gas (H_2:Ar [v:v] = 2.8:97.2). The H_2 concentration can be tuned as 0 to 2.8% by changing the pure argon and argon–hydrogen mixture gas ratio during TCO film deposition process. The base vacuum pressure of the chamber was 2×10^{-4} Pa, and the pressure for the sputtering process was set as 0.78 Pa. No additional heating on substrate was applied during deposition. We use rotary targets for film deposition, and the power density was set as 4 kW/m.

2.2 | SHJ solar cells

The structural schematic of double-side SHJ solar cells is illustrated in Figure 1A. Commercial n-type (100) oriented Czochralski (CZ) silicon wafers of 160 μm thickness and resistivity of 1 Ω·cm was used in this work. As-cut wafers first undergo wet-chemical process including saw-damage removal, texturing and cleaning. After cleaning, 7-nm a-Si:H(i) was deposited as passivation layer on both sides of the wafer. The 25-nm μ-Si:H(n^+) (or 7-nm a-Si:H(n^+)) and 10-nm a-Si:H(p^+) were deposited as the front contact layer and rear emitter. All a-Si:H and μ-Si:H layers were deposited using home-made plasma enhanced chemical vapor deposition (PECVD) equipment. The main PECVD deposition parameters are listed in Table 1. Then, 80-nm TCO films were sputtered on the both sides of the sample, and Ag grids were printed on both sides. After screen printing, the solar cells were annealed at 190°C for 20 min. Figure 1B,C shows TEM images of the front structure of SHJ solar cell on a non-textured silicon wafer. The μ-Si:H(n^+) and IMO:H were deposited on the silicon wafer, which were prepared using the same experimental condition as the real cell. A clearer image of μ-Si:H(n^+) and IMO:H is shown in Figure S1. As can be seen, both μ-Si:H(n^+) and IMO:H film show the crystallization to a certain extent. The grain size of μ-Si:H(n^+) films is several nanometers. The structure of SHJ solar cell is Ag grids/IMO:H (or ITO)/μ-Si:H(n^+) (or a-Si:H(n^+))/a-Si:H(i)/n-type c-Si/a-Si:H(i) /a-Si:H(p^+)/ITO/Ag grids. The cell area is 274.5 cm^2.

2.3 | Characterization

The optical transmission and reflection spectra was measured on a spectrophotometer (PerkinElmer Lambda1050). The cross-sectional TEM lift-out samples were fabricated using an FEI Helios NanoLab G4 CX focused ion beam microscope. The cross-sectional images were observed by TEM (FEI-F20). Sheet resistance of films was measured using a four-point probe method. The Cox and Strack method was used to evaluate the contacts resistivity on SHJ silicon solar cells. Quantum efficiency (BENTHAM INSTRUMENT PVE300-IVT) spectra was measured to study the spectral response of the fabricated cells.

3 | RESULTS AND DISCUSSION

As we know, hydrogen doping significantly improves the performance of the TCO films.[20] Therefore, the relationship between hydrogen concentration in the sputtering gas and the properties of IMO:H films was explored. The 115-nm-thick IMO:H films were sputtered on glass substrates. The XRD pattern is provided in Figure S2. Figure 2A shows their effective total transmittance spectra. The effective total transmittance (*TT*e) is defined as follows:

$$TTe = \frac{T}{(1-R)} \quad (1)$$

where T is the absolute transmittance of the film and R is the absolute reflectance. *TT*e is used to evaluate film absorption without influence of reflection.[21] As can be seen in Figure 2A, with the increasing of H_2 concentration, the transmittance of IMO:H films increased firstly and then decreased. When H_2 concentration is relatively low (≤1.5%), the

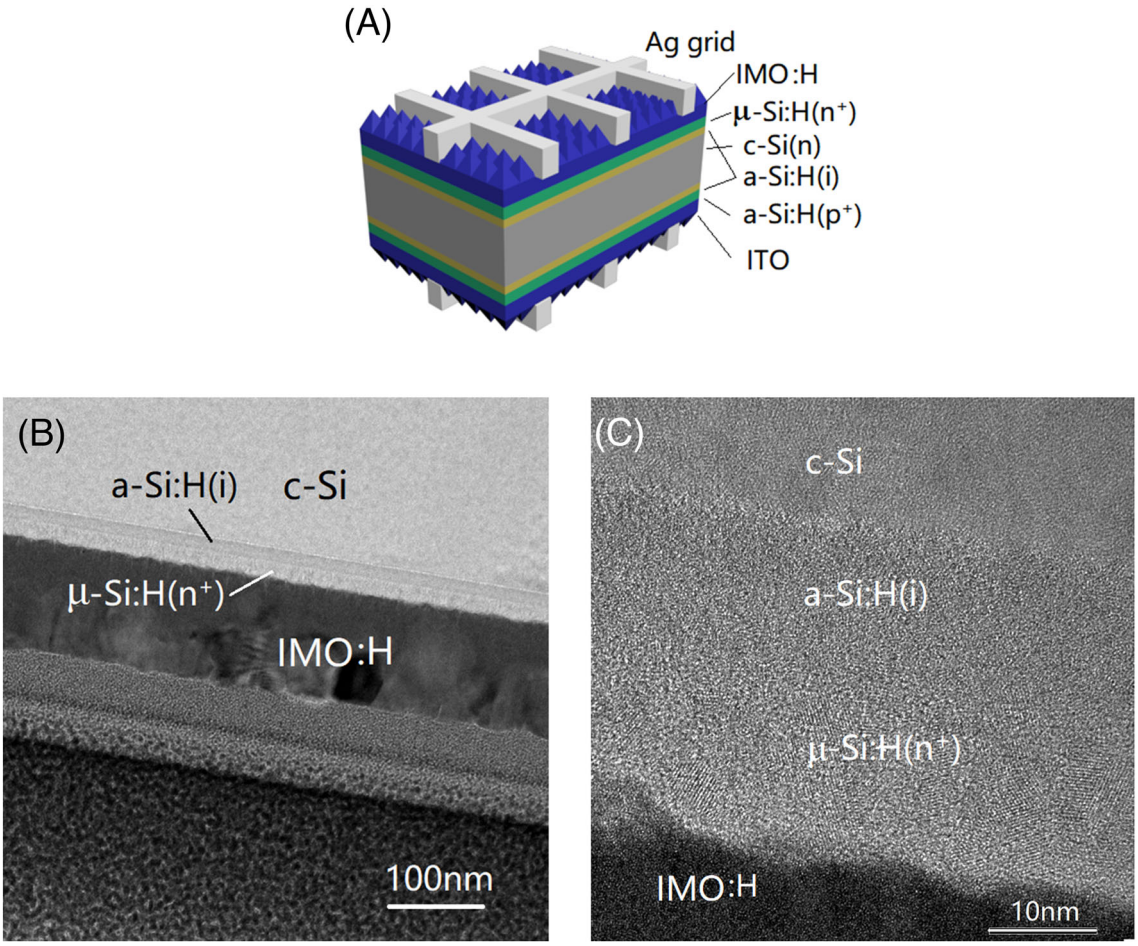

FIGURE 1 (A) Structural schematic of the silicon heterojunction (SHJ) solar cells. (B, C) Cross-sectional TEM images taken at the front structure of SHJ solar cell

TABLE 1 PECVD deposition parameters

Layer	Thickness (nm)	Temperature (°C)	Pressure (mBar)	Power density (mW/cm^2)	Power supply
a-Si:H(i)	7	210	0.65	12	RF (13.56 MHz)
a-Si:H(p$^+$)	10	150	0.8	18	RF (13.56 MHz)
a-Si:H(n$^+$)	7	190	0.65	18	RF (13.56 MHz)
μ-Si:H(n$^+$)	25	190	3	260	VHF (40.68 MHz)

average transmittance of IMO:H films was higher than that of the ITO film especially in the short wavelength region, this indicates a larger bandgap for IMO:H films (seen Figure S3). It should be noted that as the H_2 concentration increased to 2.8%, the transmittance of IMO:H film is much lower than that of ITO film. Meanwhile, the absorptance of IMO:H films increased with the increase of H_2 concentration in the near- infrared (NIR) region. According to the Drude model,[8,19] the NIR free carrier absorption (FCA) is related to carrier concentration, so the IMO:H films with a higher H_2 concentration become less transparent as they have higher carrier concentration, which can be verified in Figure 2C.

Figure 2B–D shows the sheet resistance, carrier concentration, and Hall mobility of IMO:H and ITO films. The 89.31 Ω/□ sheet resistance of ITO film is provided as a reference. This sheet resistance of ITO is an optimized parameter, which has been verified by mass production of a-Si:H(n$^+$) SHJ solar cells in our company's pilot production line. Previously, a certificated total area efficiency of 24.78% had been achieved on this type of ITO/a-Si:H(n$^+$) SHJ solar cell, see Figure S4. With the increase of H_2 concentration, the sheet resistance of IMO:H films decreased firstly and then increased. It reached the lowest value (29.94 Ω/□) at 1% H_2 concentration. As we know, the sheet resistance is inversely proportional to the free carrier concentration and

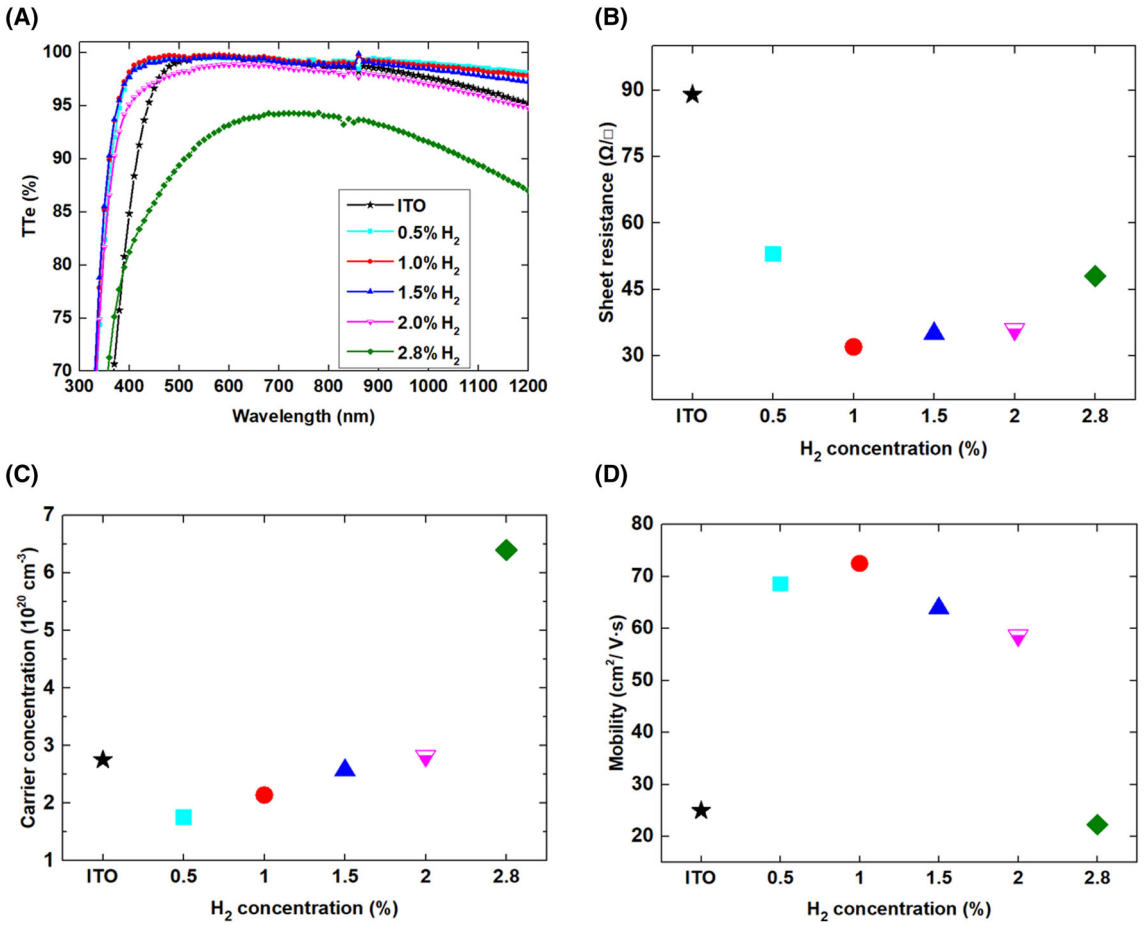

FIGURE 2 (A) The effective total transmittance of IMO:H and indium tin oxide (ITO) films; here we fixed O_2/Ar ratio at 1.9% for all samples. (B) Sheet resistance, (C) carrier concentration, and (D) mobility for IMO:H and ITO films

Hall mobility. It is obvious that the sheet resistance decreases with the increase of H_2 concentration from 0.5% to 1% due to the increase of the free carrier concentration and Hall mobility. The mobility of IMO:H is higher than that of ITO at low H_2 concentration (≤2%). It reached by 72.5 $cm^2/V{\cdot}s$ at 1.0% H_2 concentration and then decreased quickly down to 21.90 $cm^2/V{\cdot}s$ for higher hydrogen concentration. The relationship between mobility and H_2 concentration can be attributed to the minimization of charged and neutral impurity scattering by hydrogen doping.[22,23] Early studies have indicated that hydrogen in TCO materials acts as an effective donor.[7,24–26] As expected, the carrier concentration increased continuously with the H_2 concentration increasing (Figure 2C). At low H_2 concentration range (0.5%–1.5%), the carrier concentration of IMO:H is lower than that of ITO. As a TCO material for SHJ solar cells, too high carrier concentration is sometimes not expected. It brings high FCA, which in turn leads to the low *TT*e of IMO:H films with high H_2 concentration as shown in Figure 2A. By analyzing transmittance, sheet resistance, carrier concentration and mobility results, we suggest that the appropriate hydrogen concentration is 1%–1.5%.

In order to achieve lower series resistance and higher *FF* of solar cells, reducing contact resistivity between different layers is very important. The Cox and Strack configuration was used for contact resistivity measurement.[27,28] The total resistance can be written as follows:

$$R_t - R_s = R_c + R_0 \tag{2}$$

$$R_s = \frac{\rho}{d\pi}\arctan\frac{4t}{d} \tag{3}$$

$$R_c = \frac{4\rho_c}{\pi d^2} \tag{4}$$

where R_t, R_s,R_c, and R_0 represent total resistance, spreading resistance, contact resistance, and residual resistance, respectively, ρ and t are the resistivity and thickness of Si substrate, d is the diameter of circle electrode, and ρ_c is the contact resistivity. The contact resistivity between IMO:H and a-Si:H(n^+) or μ-Si:H(n^+) was studied. For comparison, the contact resistivities between conventional ITO and a-Si:H (n^+) or μ-Si:H(n^+) were also measured. The details and structures of devices 1#–4# are shown in Table 2 and Figure 3A. The rear structure is a-Si:H(i)/μ-Si:H(n^+)/IMO:H/Al (Figure 3A) and is the same for all devices. Circular front electrodes with 3-, 4-, 5-, 6-, 7-, and 8-mm diameter were deposited for the Cox and Strack configuration.

Figure 3B shows the I-V curves of device 1#. All of them are almost linear. ρ_c is the slope of $(R_t - R_s)$ versus $4(\pi d^2)^{-1}$ curve according to formulas 2 and 4. The fitting results are given in Figure 3C. The ρ_c of different front stacked structures were also given in Table 2. The combination of IMO:H and μ-Si:H(n^+) has the lowest contact resistivity of 17 mΩ·cm^2. It is noted that the ρ_c of ITO and a-Si:H(n^+) is also low. That's why ITO was chosen for SHJ cell with a-Si:H windows layer.[29,30]

Figure 4 shows the open-circuit voltage (V_{OC}), short current density (J_{sc}), fill factor (*FF*), and efficiency (E_{ff}) of SHJ solar cells with the two selected front structures of IMO:H + μ-Si:H(n^+) and ITO + a-Si:H (n^+). The average E_{ff} of solar cells with IMO:H + μ-Si:H(n^+) is improved by 0.4% compared with that of the solar cells with ITO + a-Si:H(n^+). It is mainly due to the significant increase of J_{sc} and FF, which is further attributed to the higher transmittance of IMO:H (and μ-Si:H(n^+)) layer and the lower contact resistance between IMO:H and μ-Si:H(n^+) layer.[16,18]

TABLE 2 Contact resistivity between different TCOs and n-type silicon layers

	Contact layer	TCO	Contact resistivity (mΩ·cm^2)
1#	μ-Si:H(n^+)	IMO:H	17.4
2#	a-Si:H(n^+)	IMO:H	606.8
3#	a-Si:H(n^+)	ITO	77.7
4#	μ-Si:H(n^+)	ITO	92.1

Subsequently, SHJ solar cells were sent to ISFH CalTeC for the performance certification. The champion E_{ff} of 25.26% was achieved on the SHJ solar cell with a MgF_2 + IMO:H + μ-Si:H(n^+) front contact layer (Figure 5). It is worth mentioning that the J_{sc} exceeds 40 mA/cm^2 for a SHJ solar cell with screen printed Ag grids. It is a high value for a SHJ solar cell since Kaneka reported a 40.1 mA/cm^2 current density for a SHJ solar cell by means of copper electroplating technology.[31] Compared with Ru's work[5] (SHJ solar cell with ITO +- μ-Si:H(n^+)), the J_{sc} of our SHJ solar cell increased by 0.45 mA/cm^2, which can be mainly attributed to contribution of the IMO:H layer.

Figure 6 displays the external quantum efficiency (EQE) for the two types of SHJ solar cells, that is, with the MgF_2 + IMO:H + μ-Si:H (n^+) and MgF_2 + ITO + a-Si:H(n^+) front contact, respectively. The EQE data here are from the SHJ solar cells certified in ISFH CalTeC (see Figures 6 and S4). The *TT*e spectra of μ-Si:H(n^+) and a-Si:H(n^+) are also provided. The EQE of solar cell with IMO:H + μ-Si:H(n^+) is higher than that of solar cell with ITO + a-Si:H(n^+) in both short and long wavelength reigns. We suggested that it is due to the high transmittance of IMO:H and μ-Si:H(n^+) at short and long wavelength in IMO:H as shown in Figures 6 and 2A.

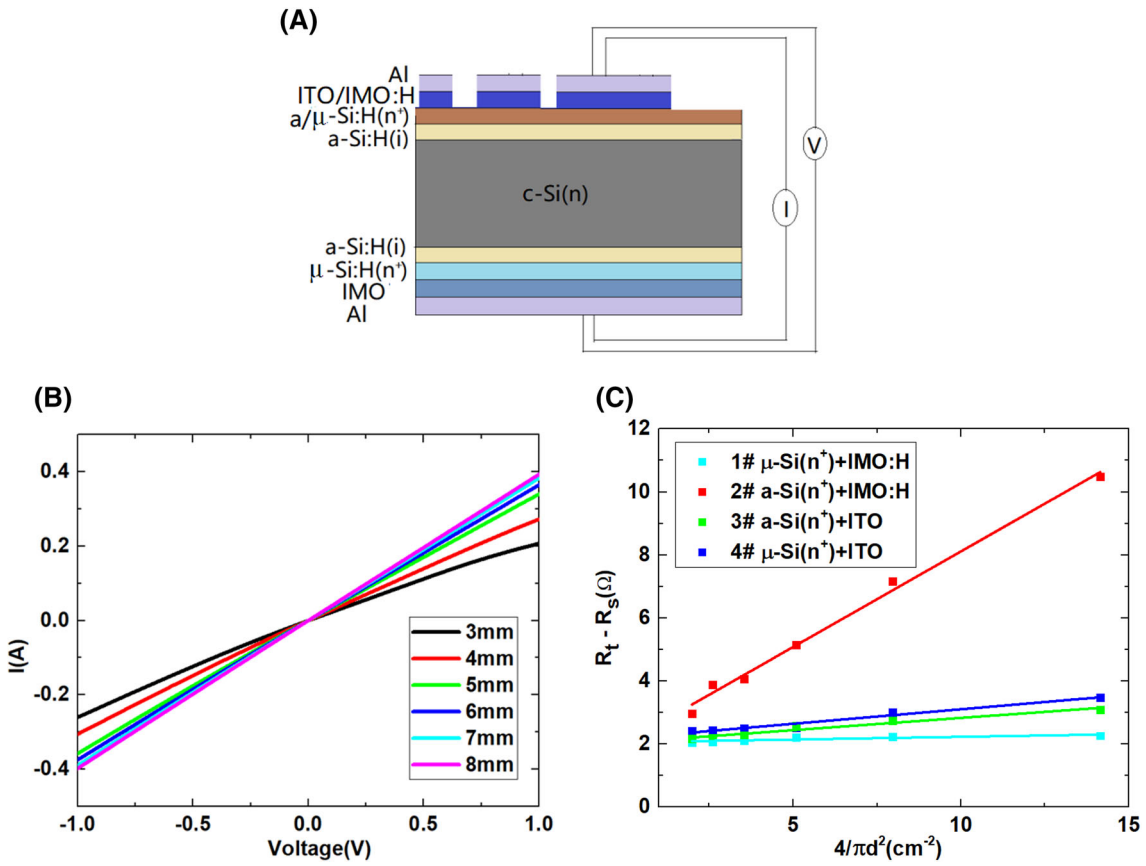

FIGURE 3 (A) Schematic of the Cox and Strack configuration of the samples used for contact resistivity measurements. (B) I-V curves for different contact area. (C) Slope fitting for contact resistivity evaluation

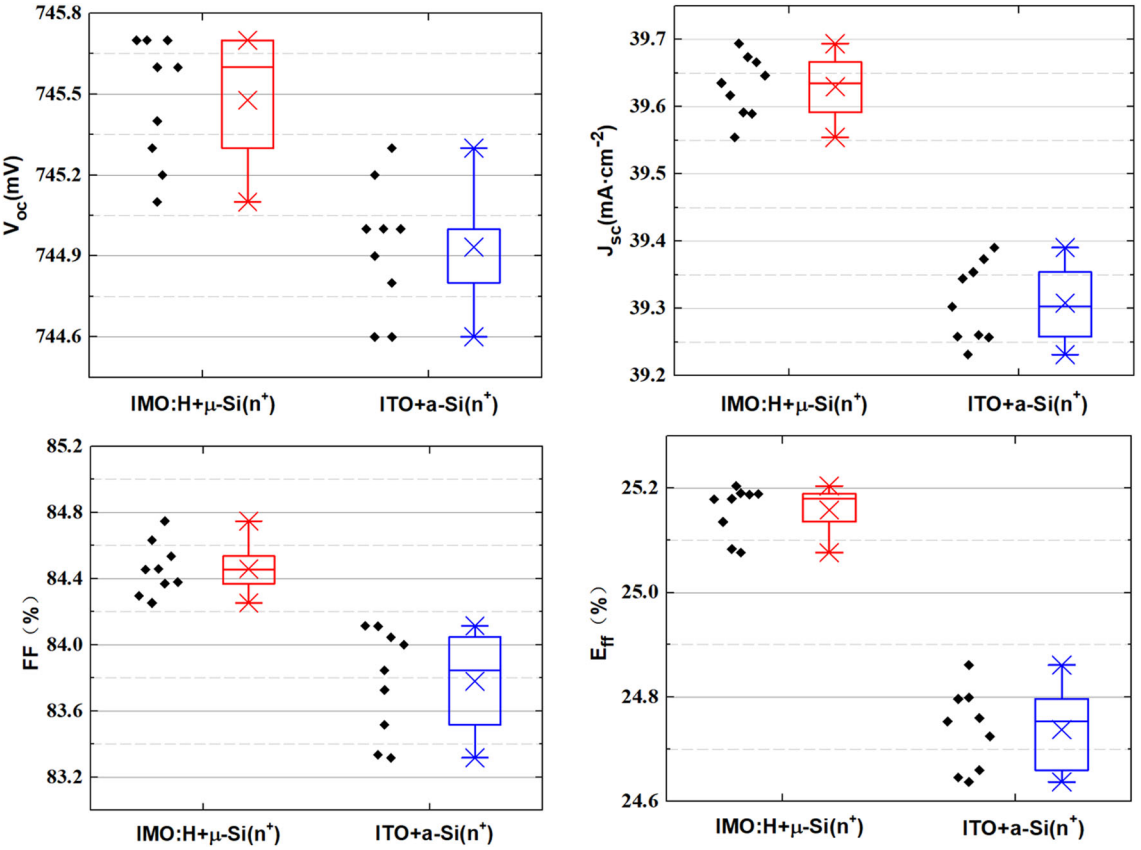

FIGURE 4 The photovoltaic parameters of silicon heterojunction (SHJ) solar cells with different front contacts and transparent conductive oxide (TCO) films

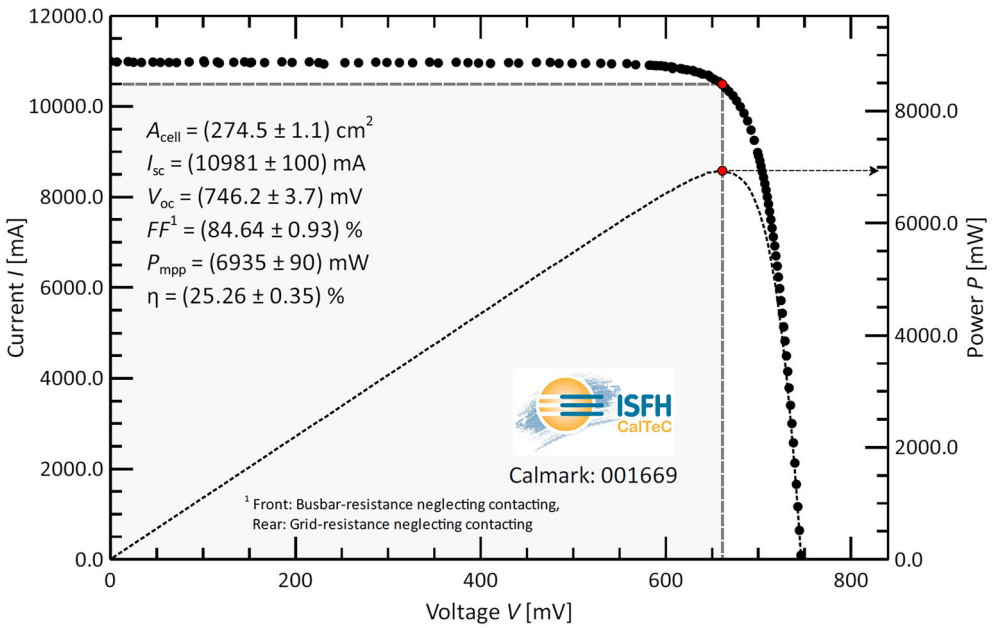

FIGURE 5 The light I-V curves of champion silicon heterojunction (SHJ) solar cell. The photograph of the SHJ solar cell is provided in Figure S5

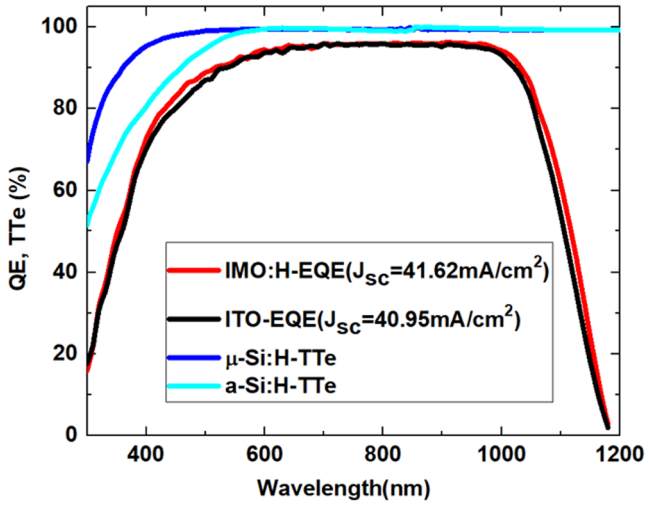

FIGURE 6 The external quantum efficiency (EQE) of silicon heterojunction (SHJ) solar cells with MgF_2 + IMO:H + μ-Si:H(n^+) and MgF_2 + ITO + a-Si:H(n^+) front contact layers. The *TTe* spectrum of μ-Si:H(n^+) and a-Si:H(n^+) is provided for comparison

4 | CONCLUSIONS

In summary, high-quality IMO:H thin films were deposited by magnetron sputtering method. The effective total transmittance, sheet resistance, carrier concentration, and mobility for IMO:H films were investigated as a function of hydrogen concentration. Among them, IMO:H films prepared with 1% hydrogen concentration in the sputtering gas showed a high Hall mobility of 72.5 $cm^2/V{\cdot}s$ and a relatively high transmittance in the wavelength region of 300–1200 nm. The contact resistivity between IMO:H film and μ-Si:H(n^+) was 17.4 $m\Omega{\cdot}cm^2$, which is lower than that of other TCOs and n layers combination. Attributed to the good optical and electrical properties of IMO:H and μ-Si:H(n^+) layer, the performance of SHJ solar cells with IMO:H film and μ-Si:H(n^+) front contact layer were improved significantly compared with the typical SHJ solar cells with an ITO and a-Si:H(n^+) front contact layer. EQE enhancement in short and long wavelength regions leads to an increase in J_{sc} of 0.67 mA/cm^2. Finally, a 25.26% (total area 274.5 cm^2) efficiency SHJ solar cell with high J_{sc} exceeding 40 mA/cm^2 was achieved.

ACKNOWLEDGEMENTS

Thanks so much to Tianwei Tang, Xiaochao Ran, Chenran He, Si Huang, Hongfan Wu, and Hao Jiang for discussion and sample preparation.

ORCID

Yurong Zhou https://orcid.org/0000-0003-4947-0612

REFERENCES

1. Taguchi M, Kawamoto K, Tsuge S, et al. HITTM cells-high-efficiency crystalline Si cells with novel structure. *Prog Photovoltaics: Res Appl*. 2000;8(5):503-513. doi:10.1002/1099-159X(200009/10)8:5<503::AID-PIP34>3.0.CO;2-G
2. Taguchi M, Yano A, Tohoda S, et al. 24.7% record efficiency HIT solar cell on thin silicon wafer. *IEEE J Photovolt*. 2013;4(1):96-99. doi:10.1109/JPHOTOV.2013.2282737
3. Ruan T, Qu M, Wang J, et al. Effect of deposition temperature of a-Si:H layer on the performance of silicon heterojunction solar cell. *J Mater Sci Mater Electron*. 2019;30(14):13330-13335. doi:10.1007/s10854-019-01700-7
4. Yoshikawa K, Kawasaki H, Yoshida W, et al. Silicon heterojunction solar cell with interdigitated back contacts for a photoconversion efficiency over 26%. *Nat Energy*. 2017;2(5):1-8. doi:10.1038/nenergy.2017.32
5. Ru X, Qu M, Wang J, et al. 25.11% efficiency silicon heterojunction solar cell with low deposition rate intrinsic amorphous silicon buffer layers. *Sol Energy Mater sol Cells*. 2020;215:110643. doi:10.1016/j.solmat.2020.110643
6. Richter A, Benick J, Feldmann F, Fell A, Hermle M, Glunz SW. n-Type Si solar cells with passivating electron contact: Identifying sources for efficiency limitations by wafer thickness and resistivity variation. *Sol Energy Mater sol Cells*. 2017;173:96-105. doi:10.1016/j.solmat.2017.05.042
7. Koida T, Fujiwara H, Kondo M. Hydrogen-doped In2O3 as high-mobility transparent conductive oxide. *Jpn J Appl Phys*. 2007;46(7L):L685-L687. doi:10.1143/JJAP.46.L685
8. Koida T, Kondo M, Tsutsumi K, Sakaguchi A, Suzuki M, Fujiwara H. Hydrogen-doped In 2 O 3 transparent conducting oxide films prepared by solid-phase crystallization method. *J Appl Phys*. 2010;107(3):033514. doi:10.1063/1.3284960
9. Diniz ASAC. The effects of various annealing regimes on the microstructure and physical properties of ITO (In_2O_3: Sn) thin films deposited by electron beam evaporation for solar energy applications. *Renew Energ*. 2011;36(4):1153-1165. doi:10.1016/j.renene.2010.09.005
10. El-Nahass MM, El-Menyawy EM. Thickness dependence of structural and optical properties of indium tin oxide nanofiber thin films prepared by electron beam evaporation onto quartz substrates. *Mater Sci Eng, B*. 2012;177(2):145-150. doi:10.1016/j.mseb.2011.10.018
11. de Carvalho CN, Luis A, Conde O, et al. Effect of rf power on the properties of ITO thin films deposited by plasma enhanced reactive thermal evaporation on unheated polymer substrates. *J Non Cryst Solids*. 2002;299:1208-1212. doi:10.1016/S0022-3093(01)01140-1
12. de Carvalho CN, Lavareda G, Fortunato E, Nunes de Carvalho C, Amaral A. Properties of ITO films deposited by rf-PERTE on unheated polymer substrates—dependence on oxygen partial pressure. *Thin Solid Films*. 2003;427(1-2):215-218. doi:10.1016/S0040-6090(02)01213-0
13. Zuev DA, Lotin AA, Novodvorsky OA, et al. Pulsed laser deposition of ITO thin films and their characteristics. *Sem Ther*. 2012;46(3):410-413. doi:10.1134/S1063782612030256
14. Izumi H, Ishihara T, Yoshioka H, Motoyama M. Electrical properties of crystalline ITO films prepared at room temperature by pulsed laser deposition on plastic substrates. *Thin Solid Films*. 2002;411(1):32-35. doi:10.1016/S0040-6090(02)00169-4
15. Shi J, Shen L, Meng F, Liu Z. Structural, electrical and optical properties of highly crystalline indium tin oxide films fabricated by RPD at room temperature. *Mater Lett*. 2016;182:32-35. doi:10.1016/j.matlet.2016.06.084
16. Yu C, Yang M, Dong G, et al. Development of silicon heterojunction solar cell technology for manufacturing. *Jpn J Appl Phys*. 2018;57(8S3):08RB15. doi:10.7567/JJAP.57.08RB15
17. Koida T, Fujiwara H, Kondo M. High-mobility hydrogen-doped In_2O_3 transparent conductive oxide for a-Si: H/c-Si heterojunction solar cells. *Sol Energy Mater sol Cells*. 2009;93(6–7):851-854. doi:10.1016/j.solmat.2008.09.047
18. Barraud L, Holman ZC, Badel N, et al. Hydrogen-doped indium oxide/indium tin oxide bilayers for high-efficiency silicon

heterojunction solar cells. *Sol Energy Mater sol Cells*. 2013;115:151-156. doi:10.1016/j.solmat.2013.03.024
19. Kondo K, Yoshida S, Ono H, Abe M. Spin sprayed Ni (–Zn)–Co ferrite films with natural resonance frequency exceeding 3 GHz. *J Appl Phys*. 2007;101(9):09M502. doi:10.1063/1.2710465
20. Huang M, Hameiri Z, Aberle AG, Mueller T. Study of hydrogen influence and conduction mechanism of amorphous indium tin oxide for heterojunction silicon wafer solar cells. *Phys Status Solidi a*. 2015;212(10):2226-2232. doi:10.1002/pssa.201532221
21. Yu C, Yang M, Zhang Y, et al. Development of high efficiency rear-emitter n-type silicon heterojunction solar cells. In: *2015 IEEE 42nd Photovoltaic Specialist Conf (PVSC)*. IEEE; 2015:1-5.
22. Morales-Masis M, De Wolf S, Woods-Robinson R, Ager JW, Ballif C. Transparent Electrodes for Efficient Optoelectronics. *Adv. Electron Mater*. 2017;3(5):1600529. doi:10.1002/aelm.201600529
23. Chen M, Pei ZL, Wang X, et al. Intrinsic limit of electrical properties of transparent conductive oxide films. *J Phys D Appl Phys*. 2000;33(20):2538-2548. doi:10.1088/0022-3727/33/20/304
24. McCluskey MD, Tarun MC, Teklemichael ST. Hydrogen in oxide semiconductors. *J Mater Res*. 2012;27(17):2190-2198. doi:10.1557/jmr.2012.137
25. King PDC, Lichti RL, Celebi YG, et al. Shallow donor state of hydrogen in In_2O_3 and SnO_2: Implications for conductivity in transparent conducting oxides. *Phys Rev B*. 2009;80(8):081201. doi:10.1103/PhysRevB.80.081201
26. Omura H, Kumomi H, Nomura K, Kamiya T, Hirano M, Hosono H. First-principles study of native point defects in crystalline indium gallium zinc oxide. *J Appl Phys*. 2009;105(9):093712. doi:10.1063/1.3089232
27. Cox RH, Strack H. Ohmic contacts for GaAs devices. *Solid State Electron*. 1967;10(12):1213-1218. doi:10.1016/0038-1101(67)90063-9
28. Tanahashi T, Sakamoto N, Shibata H, Masuda A. Corrections to "Corrosion-induced ac impedance elevation in front electrodes of crystalline silicon photovoltaic cells within field-aged photovoltaic modules". *IEEE J Photovoltaics*. 2019;9(4):1154-1154. doi:10.1109/JPHOTOV.2019.2914944
29. Dong G, Hong C, Cui G, et al. Water vapor doped TCO films and application to silicon heterojunction solar cells. *2018 IEEE 7th World Conference on Photovoltaic Energy Conv (WCPEC), IEEE*. 2018;2121-2125.
30. Gong W, Wang G, Gong Y, et al. Investigation of In_2O_3: SnO_2 films with different doping ratio and application as transparent conducting electrode in silicon heterojunction solar cell. *Sol Energy Mater sol Cells*. 2022;234:111404. doi:10.1016/j.solmat.2021.111404
31. Adachi D, Hernández J L, Yamamoto K. Impact of carrier recombination on fill factor for large area heterojunction crystalline silicon solar cell with 25.1% efficiency. *Appl Phys Lett*. 2015;107(23):233506. doi:10.1063/1.4937224

SUPPORTING INFORMATION

Additional supporting information may be found in the online version of the article at the publisher's website.

How to cite this article: Dong G, Sang J, Peng C-W, Liu F, Zhou Y, Yu C. Power conversion efficiency of 25.26% for silicon heterojunction solar cell with transition metal element doped indium oxide transparent conductive film as front electrode. *Prog Photovolt Res Appl*. 2022;1-8. doi:10.1002/pip.3565